The Global Atmosphere and Ocean System, Vol. 00, No. 0, pp. 1–19

Taylor & Francis
Taylor & Francis Group

THE WEATHER FORECASTING SYSTEM FOR POSEIDON – AN OVERVIEW

A. PAPADOPOULOS[a,b,*], P. KATSAFADOS[a], G. KALLOS[a] and S. NICKOVIC[c]

[a]*University of Athens, Department of Applied Physics, Panepistimioupolis Bldg. PHYS-V, Athens 15784, Greece;* [b]*National Centre for Marine Research, Institute of Oceanography, Ag. Kosmas Elliniko, 166 04 Athens, Greece;* [c]*Euro-Mediterranean Centre on Insular Coastal Dynamics (ICoD), University of Malta, Valletta, Malta*

(Received 31 August 2001)

A weather forecasting system has been developed in the framework of the POSEIDON project "Monitoring, forecasting and information system for the Greeks seas". The system is currently running operationally at the National Centre for Marine Research (NCMR) providing detailed and accurate weather forecasts. It also forces a general circulation ocean model and an offshore wave model with the surface fluxes of momentum and heat and with the precipitation rates. Because of the specific applications for marine studies and operations, emphasis was given to the surface processes especially over the water body. The system contains a viscous sublayer model, which is considered as appropriate for a flux description. The system is evaluated systematically with the aid of the POSEIDON buoy network and other meteorological information available. A description of the system and its capabilities are presented below.

Keywords: POSEIDON; National Centre for Marine Research (NCMR)

1. INTRODUCTION

An accurate prediction of the sea state has been recognized as a need for a long time, but only during the last years has it become a subject of scientific research. The science of the Operational Oceanography, especially the forecasting aspect started its first steps when the technological achievements allowed the application of sophisticated numerical models. The numerical models were restricted by the lack of real-time ocean observations. Because of their differential conservation equations temporal boundary values are required, representing an initial-value problem and when the model domain size is finite, spatial boundary information is also needed (boundary-value problem). New techniques for measuring the sea state and transmitting data in real time, in combination with the significant advancement in computer technology, allowed the development of Operational Oceanography and especially the forecasting operation in directions that a few years before seemed to be unreachable goals.

*Corresponding author.

ISSN 0000-0000 print: ISSN 0000-000X online/01/010000-00 © 2002 Taylor & Francis Ltd
DOI:

During the last decade, many organizations worldwide have developed services in the field of Operational Oceanography in the framework of national and international projects. Following this trend, NCMR set up the integrated project POSEIDON. POSEIDON is a real time monitoring and forecasting system for the marine environmental conditions in the Aegean Sea. The integrated monitoring network of the system consists of 11 Seawatch oceanographic buoys and 9 Smart wave buoys with the ability of on-line transmittance to the operational center of the NCMR every 3 h through Inmarsat-C satellite or a GSM mobile telephone communication system. Its enhanced forecasting system consists of an atmospheric model, an offshore wave model, a general circulation ocean model, a surface pollutant dispersion model and a shallow water wave model.

The POSEIDON weather forecasting system is based on the SKIRON/Eta system (Kallos *et al.*, 1997a) and has been developed in order to operate fully automatically. Its implementation requires a Unix or Linux computational environment and corresponding meteorological data input. It provides detailed and accurate weather forecasts for the needs of the NCMR. It is loosely coupled with the offshore wave models (DAUT, Christopoulos and Koutitas, 1991 and WAM-cycle 4, Komen *et al.*, 1994) and the ocean hydrodynamic model (Princeton Ocean Model, (POM), Blumberg and Mellor, 1983, Korres *et al.*, 2002). The coupling is obtained through surface fluxes of momentum and heat as well as precipitation and radiation (short wave and long wave). One major application concerns the linking with a dust uptake-transport-deposition module. The Seawatch buoy measurements are currently used for its evaluation and soon they will be used in data assimilation in order to improve the forecast skill in the area of interest.

2. THE WEATHER FORECASTING SYSTEM FOR POSEIDON

The basic concept was to design a reliable and computationally efficient system that produces forecasts, particularly useful for predicting local atmospheric conditions (including severe weather events such as excessive rainfall, gust winds, etc.) in order to provide the surface boundary conditions to the wave and the ocean hydrodynamic models. The weather forecasting system of POSEIDON consists of several modules, which are divided in four main parts: (a) the pre-processing, (b) the core SKIRON/Eta model, (c) the dust cycle model and (d) the post-processing. A quick description of these subsystems is provided below.

2.1 The Pre-Processing

In the pre-processing phase, meteorological parameters (geopotential, wind components and humidity) are used from a larger-scale atmospheric model. The system can utilize either:

- the European Centre for Medium-Range Forecasts (ECMWF), analysis and forecasts gridded data
- the National Center for Environmental Prediction (NCEP), analysis and forecasts gridded data
- or any other global, gridded model output or output from a 3 or 4-D data-assimilation system such as LAPS from NOAA/FSL.

The data are decoded and interpolated onto the SKIRON/Eta model grid-structure. In the preparation phase, surface parameters, observed or pre-defined (topography, sea surface temperature (SST), soil and vegetation types, soil temperature and wetness, slopes and the azimuths of the sloping surfaces) are calculated on the model grid. During this phase, all the parameters determining the area, the resolution and the model configuration constants are also defined. Because of the difficulties to obtain all the necessary input data, several options are available and the commonly used data sets are also available. The topographic data set used is the one provided by the US Geological Survey (USGS) with 30×30 arc s resolution. Alternatively, the 5×5 and 10×10 arc min data can be used. The vegetation data set is also available from USGS with 30×30 arc s resolution, following the SSiB classification. For soil textural class, the UNEP/FAO data set is used after its conversion from soil type to soil textural ZOBLER classes. The coverage of this data set is global and the resolution is 2×2 min. For the SST there are four options namely the latitudinal variation of predefined SST, the climatological $1 \times 1^{\circ}$ data from NCAR (mean monthly values), the ECMWF and the NCEP $1 \times 1^{\circ}$ gridded data (weekly or daily available). For the soil temperature and moisture, predefined values or interpolated ECMWF gridded data are used for the 6 soil sublayers. Alternatively, the computed soil state (soil temperature and moisture) from the previous-day cycle is utilized. In addition to these, the slopes and the azimuths of the sloping surfaces are computed and then used for the calculation of the incoming solar radiation over the sloping terrain. Albedo and surface roughness variations are also computed in the pre-processing stage as dependence on vegetation. After being initialized, the modified SKIRON/Eta model is executed over the specified forecasting period of 72 h.

2.2 The SKIRON/Eta Model

The SKIRON/Eta model is based on the Eta, which was originally developed at the University of Belgrade, with the specific objective of being applicable to regions with steep mountains. It uses a specific "step-mountain" vertical coordinate rather than the customary pressure or sigma (or hybrid) coordinate. The Eta model has been further developed at the National Center for Environmental Prediction (NCEP, former NMC) in Washington, USA since 1993. It is used as a fully operational weather forecasting model in United States, having in tests outperformed other NCEP models. During the period 1995–1997, the development of the modeling system has been undertaken at the University of Athens, in the framework of projects SKIRON and MEDUSE (Kallos *et al.*, 1997a,b; Nickovic *et al.*, 1997a,b). In the last three years, the entire system has been further developed in the framework of the POSEIDON system and it is specialized for marine applications.

Model Dynamics

The Eta model uses the primitive equations based on the hydrostatic approximation. Consequently, it can be executed with the finest horizontal resolution of about 5 km. It is formulated as a grid-point model and the partial differential equations are represented by finite-difference schemes. The numerical schemes are designed to fulfill computational economy requirements as well as physical constraints of the real atmosphere. In the horizontal, the model is defined over the semi-staggered E grid. The choice of the

E grid was based on the fact that this shows good performance in simulating smaller-scale processes (such as gravity–inertia disturbances). The method, which provides a proper behavior of the model with variables on the E grid, is developed for strong physical forcing (e.g. orography influence, convection, turbulence). Time differencing in the Eta model is performed with explicit time differencing schemes (Mesinger, 1973, 1977; Janjic, 1974, 1979). A careful attention is paid to the choice of time discretization techniques in order to provide efficient model executions. For terms related to smaller-scale processes, the forward–backward explicit scheme is used, integrating the continuity equation forward and pressure gradient terms backward in time. The forward–backward scheme is two times faster than any other explicit scheme. By applying a splitting technique, the advection terms (describing slower atmospheric motions) are calculated with several times larger time step than the adjustment step, providing higher model computational efficiency. The problem of adequate simulation of mountain effects was the matter of careful consideration from the beginning of the Eta model development. Proper representation of the mountain effects was the basic reason to introduce the Eta vertical coordinate system – a method widely accepted now from the meteorological modeling community (Mesinger, 1984; Mesinger *et al.*, 1988). The mountains in the Eta system are represented as grid-box mountain blocks. The non-slip bottom boundary condition used at the vertical sides of the model mountains provides efficient simulation of the blocking, splitting and channeling effects due to mountain influence. The second-order non-linear advection scheme is designed for the horizontal advection terms in the model equations (Janjic, 1984). This scheme conserves several important parameters such as mass, energy and squared vorticity, thus reproducing the features of the real atmosphere. Conservation properties of the scheme, therefore, prevent a false generation of the numerical noise typical for many other atmospheric models.

Model Physics

The physical package of the model represents atmospheric processes, which have smaller scales than the model grid structure and therefore, are not resolved explicitly. The physical part of the SKIRON/Eta model is based on several sophisticated parameterization schemes. Vertical turbulent mixing between levels in the free atmosphere is performed by using mixing coefficients of the Mellor–Yamada 2.5 level turbulence (Mellor and Yamada, 1974, 1982; Janjic, 1990). Vertical mixing in the surface layer is performed by a Monin–Obukhov similarity model. The introduction of a viscous sublayer (Janjic, 1994) describes a more realistic situation near the surface. Different viscous sublayer approaches are applied over ground and over water surfaces in the model. A non-linear fourth-order lateral diffusion scheme, with the diffusion coefficient depending on the deformation and the turbulent kinetic energy, is introduced to control the level of small-scale noise. For simulation of the radiative atmospheric effects, the Geophysical Fluid Dynamics Laboratory (GFDL) radiation scheme is used, which includes interactive random overlap cloud effects. This scheme is relatively efficient because it uses extensively pre-calculated values of various parameters (look-up tables) which with no effect in accuracy. The revised Betts–Miller deep and shallow cumulus convection scheme is used in order to represent moisture processes responsible for excessive precipitation events (Betts, 1986; Betts and Miller, 1986; Janjic, 1994). The large-scale condensation scheme is implemented to simulate moist atmospheric processes on larger scales. The Oregon State University (OSU) scheme for the simulation of the surface processes, including surface hydrology, is incorporated in the model. This model component provides a proper exchange of heat, moisture and momentum between the atmosphere and the earth surface. An alternative scheme is the Land Atmosphere Parameterization Scheme, LAPS, (Mihailovic and Kallos, 1997). For the surface-process calculations, a corresponding set of high resolution ground conditions (soil and vegetation types, topography, SST) is included.

2.3 The Dust Cycle Model

Saharan dust deposition over the Mediterranean waters is an important factor in various marine applications. It is believed that the deposition of Saharan dust is responsible for the supply of nutrients resulting in the increase of the production of the pelagic system, but competitively may remove phosphorus, through the adsorption on dust particles, contributing to the oligotrophy of the system. In addition, the presence of Si and Fe in the dust deposition may change the phytoplankton communities resulting in fast growth rates leading to blooms. The resultant higher fluxes of organic matter may propagate to deeper layers changing the structure of the sediments.

In order to be able to investigate all these processes, the weather forecasting system of POSEIDON was enhanced with a module able to describe the dust cycle in the atmosphere. This module was developed by the Atmospheric Modelling and Weather Forecasting group at the University of Athens (Kallos *et al.*, 1997b; Nickovic *et al.*, 1997a,b, 2001). The development has been done initially within the frame of the EU funded project MEDUSE. Further development was made for the specific needs of the POSEIDON system. The system with the dust capability is probably the first model, which is applied to operational dust alerts.

The dust modules of the entire system incorporate the state of the art parameterizations of all the major phases of the desert dust life such as production, diffusion, advection and removal. These modules also include the effects of the particle size distribution in order to simulate more accurately the size-dependent processes. Currently, there are four bins of dust particle size distribution available and they should be increased accordingly if necessary. Recent improvements and modifications of the transport part of the model are made in order to have this module available as a separate plug-in to the entire system which can be easily switched on/off according to the needs and applications (Nickovic *et al.*, 2001). A critical point in the simulation of dust concentration is the aerosol production phase. It is obvious that large deviations from real conditions during dust storms may lead to poor simulation of the dust cycle. Therefore, special care was taken to determine, as accurately as possible, the dust productivity areas. In the pre-processing phase of the weather forecasting system, before the actual model execution begins, each grid point is specified if it will act as a desert dust source according to its corresponding soil and land cover. For this purpose, the high-resolution data sets of vegetation and soil and texture types that are utilized for the preparation of the input data for the atmospheric driving model are also used for the specification of dust sources and for the calculation of dust-related processes dependent on soil conditions. During the model run, the prognostic atmospheric and hydrological conditions are used in order to calculate the effective rates of the injected dust concentration based on the viscous/turbulent mixing, shear-free convection diffusion and soil moisture.

2.4 The Post-Processing

The main products of the system are precipitation, snowfall, cloud coverage, temperature at 2 m, wind speed at 10 m, mean sea level pressure, fog, dust concentration and deposition, as well as air temperature, wind speed and geopotential height at specific standard pressure levels. One part of the post-processing is the graphics representation of the results. All the abovementioned products are plotted using for each of them a different graphics pre-processor and are available through Internet. Software has been developed in order to process the model results and prepare all the necessary input for the wave and the ocean hydrodynamic models, which operate in NCMR. In this post-processing package, various parameters from the viscous sublayer are also dumped in order to be used in the coupling with the other components of POSEIDON.

2.5 Calculation of the 10 m Wind

For the specific marine applications within the POSEIDON project, the model estimates the various fluxes, such as short and long wave radiation at the surface, sensible and latent heat fluxes and the net radiation budget at the surface. Special care is taken in the calculations of the 10 m wind, which is considered as important for the ocean circulation and wave modeling.

The relatively high vertical resolution applied in the SKIRON/Eta model, permits the application of a surface layer model based on the well established Monin–Obukhov similarity theory (Monin and Obukhov, 1954). The Monin–Obukhov surface layer parameterization scheme provides the lower boundary conditions for the Level 2.5 turbulence model and the calculations to derive wind speed and direction at 10 m above surface. In order to calculate surface turbulent flux for momentum, boundary conditions at two levels, z_1 and z_2 in the air are required. According to the similarity theory, fluxes between the two levels are assumed constant. The turbulent flux for momentum, M, is given by:

$$M = -\overline{u'w'} = K_M \frac{dU}{dz} \tag{1}$$

where K_M is the exchange coefficients for momentum. The friction velocity

$$u_* \equiv \sqrt{M} \tag{2}$$

is usually used. After integrating (1) from z_1 to z_2, it can be obtained:

$$U_2 - U_1 = M \int_{z_1}^{z_2} \frac{dz}{K_M} \tag{3}$$

According to the similarity theory, within the surface layer it is valid to submit:

$$\frac{\partial U}{\partial z} = \frac{u_*}{\kappa z} \varphi_M(\zeta) \tag{4}$$

where, ϕ_M is an empirically determined function, and

$$\zeta = \frac{z}{L} \tag{5}$$

is the nondimensional combination of geometrical height and the Monin–Obukhov length scale, $L = (M^{3/2}/\kappa\beta H_v)$, where $\beta = (1/\Theta_0) \approx (1/273\,\mathrm{K})$, Θ_0 is the ambient potential temperature, κ is the von Karman constant $(=0.4)$ and g is gravity. Integration of (4) leads to

$$U_2 - U_1 = \int_{z_1}^{z_2} \frac{u_*}{\kappa z} \varphi_M(\zeta)\, dz \tag{6}$$

Assuming constant fluxes within the surface layer, using (5) and considering the singularity in the neutral case, when L tends to zero (so ζ tends to infinity), (6) can be rewritten as:

$$U_2 - U_1 = \frac{u_*}{\kappa} \int_{\zeta_1}^{\zeta_2} [\varphi_M(\zeta) - \varphi_M(0)] \frac{d\zeta}{\zeta} + \varphi_M(0) \int_{z_1}^{z_2} \frac{dz}{z} \tag{7}$$

Since the function $\varphi_M(\zeta)$ is known, the integral on the right hand side of (7) can be evaluated as:

$$\gamma_M = \psi_M(\zeta_2) - \psi_M(\zeta_1) + \varphi_M(0) \ln\left(\frac{z_1}{z_2}\right) \tag{8}$$

Thus, (7) can be rewritten as

$$U_2 - U_1 = \frac{u_*}{\kappa} \gamma_M \tag{9}$$

In the SKIRON/Eta model, the stability functions ϕ_M and integral functions ψ_M (and then γ_M) are defined differently over land and over the water surfaces. Over the water surfaces, the functions are consistent with the Mellor–Yamada Level 2 model (Lobocki, 1993), assuming that the turbulence is extinguished for bulk Richardson numbers exceeding 0.19. Over land, the Paulson (1970) functions are used.

Using (9) the u and v components of wind velocity at 10 m above the surface can be obtained by the form:

$$U_{10} = U_{z_U} + \frac{u_*}{\kappa} \gamma_M \tag{10}$$

corresponding z_1 to the roughness height of momentum, z_U, and z_2 to a height of 10 m above the surface for momentum, thus $z_{U10} = z_U + 10$. The values of z_U, z_{U10} (necessary for the calculation of the γ_M function), u_* and U_{z_U} are calculated using a viscous sublayer defining a level near the surface where the transfer of the dependent variables by molecular motions becomes important.

In the SKIRON/Eta model the viscous sublayer is designed by matching the log profile of the considered variables with a separate viscous sublayer profile. Specifying the height and the values of the variables at that matching point, the lower boundary values for the turbulent layer can be defined. The viscous sublayer formulation described below is the one proposed by Janjic (1994). Following Liu *et al.* (1979), in the immediate vicinity of a smooth surface, the profile for the momentum can be assumed as:

$$U_1 - U_s = D_1\left[1 - \exp\left(-\frac{z_U \cdot u_*}{D_1 \cdot \nu}\right)\right]\frac{M}{u_*} \tag{11}$$

Here, the subscript s denotes the surface values, the subscript 1 denotes the values at height z_1 above the surface where the molecular diffusivities are still dominant, D_1 is a parameter to be discussed later, ν is the molecular diffusivity for momentum and M is the turbulent flux for momentum above the viscous sublayer.

With the assumption that the term $(z_U \cdot u_*/D_1 \cdot \nu) = \xi$ is approximately the value of the exponent, (11) can be approximated by:

$$U_1 - U_s = \frac{z_U}{\nu} M \tag{12}$$

The height z_U, is defined as:

$$z_U = \frac{\xi \cdot \nu \cdot D_1}{u_*} \tag{13}$$

and is assumed to be the depth of the viscous sublayer for the momentum for a chosen fixed value of ξ. In the above definitions, the value of the relevant physical quantity at the interfaces of the viscous and the turbulent layers is that denoted by the subscript 1 in (12). Another simplifying modeling assumption is taken into account, the existence of two distinct layers: (i) a thin viscous sublayer immediately above the surface, where the vertical transports are determined entirely by the molecular motion, and (ii) a turbulent layer above it, where the vertical transports are defined entirely by the turbulent fluxes.

The turbulent flux of momentum in the surface layer above the viscous sublayer, using the bulk momentum exchange coefficients K_{Mbulk}, is represented by

$$M = \frac{K_{\mathrm{Mbulk}}}{\Delta z}(U_{lm} - U_1) \tag{14}$$

where the subscript lm denotes the variable at the lowest model level and $\Delta z = z_{lm} - z_1$. Substituting (14) into (12) and solving for U_1, we get

$$U_1 = \frac{U_s + (K_{\mathrm{Mbulk}} \cdot z_u/\nu \cdot \Delta z) \cdot U_{lm}}{1 + (K_{\mathrm{Mbulk}} \cdot z_u/\nu \cdot \Delta z)} \tag{15}$$

So the required lower boundary conditions for the turbulent layer are expressed as weighted means of the values at the surface and the lowest model level.

Over the ocean, the viscous sublayer is assumed to operate in three different regimes: (i) smooth and transitional, (ii) rough and (iii) very rough with spray, depending on the Reynolds number $\mathrm{Re} = (z_0 u_*/\nu)$ where the roughness height is defined by:

$$z_0 = \max\left(0.018\frac{u_*^2}{g}, \quad 1.59 \times 10^{-5}\right) \tag{16}$$

Since, Re is a monotonic function of u_* the transitions between the regimes are assumed to occur at u_{*r}=0.025 m s^{-1} and u_{*s}=0.7 m s^{-1}, instead of in terms of Re. When u_* exceeds the value of u_{*r} the flow ceases to be smooth and the rough regime is entered. In the rough regime, the momentum is transported also by pressure forces on the roughness elements so that (11) looses its validity. Consequently, the viscous sublayer for momentum is turned off. However, for heat and moisture the viscous sublayer is still operating until the rough regime with spray is reached at the critical value u_{*s} when the viscous layer collapses completely. In the rough regime with spray, the breaking waves and the spray are assumed to provide a much more efficient way of exchange of heat and moisture between the ocean and the air than can be accomplished by the molecular viscosity.

For the parameter D_1 Liu *et al.* (1979) suggest

$$D_1 = G\mathrm{Re}^{1/4} \tag{17}$$

where G is a constant depending on flow regimes. So, Eq. (13) takes the form:

$$z_U = \xi \cdot \nu \cdot \frac{G(z_0 u_*/\nu)^{1/4}}{u_*} \tag{18}$$

In the SKIRON/Eta model, $G = 30$ is used for the smooth regime, following Liu *et al.* (1979) and when the flow ceases to be smooth, $G = 10$ is applied, which fits well with the Mangarella *et al.* (1973) data. The molecular viscosity for momentum is $\nu = 0.000015$, ξ is set as 0.35 and u_* is computed as:

$$u_* = \sqrt{\frac{K_{Mbulk}}{\Delta z}(U_{lm} - U^p_{Z_U})} \tag{19}$$

using K_{Mbulk} and $U^p_{Z_u}$ from the previous time step. Using (16), z_0 is updated with the new values of u_*.

With z_U being calculated from (18), the lower boundary conditions U_1 may be specified from (15) using K_{Mbulk} from the previous time step. In order to prevent the two-grid-interval oscillation in time, the average values of U_1 from the present and the previous time step are used. In order to calculate U_{Z_U}, Eq. (15) is rewritten in the form of:

$$U_{Z_U} = \frac{1}{2}\left[\frac{(K_{Mbulk} \cdot z_u)/(\nu \cdot \Delta z)}{1 + (K_{Mbulk} \cdot z_u)/\nu \cdot \Delta z} \cdot U_{lm} + U^p_{Z_U}\right] \tag{20}$$

where $U^p_{Z_U}$, is the value of U_{Z_U} that has been calculated at the previous time step. Therefore, since γ_M can be defined and as long as z_U is calculated by (18), z_{U10} is equal with $z_U + 10$ and U_{Z_U} is calculated using (20), the wind components at 10 m height can be computed by (10).

3. THE OPERATIONAL USE OF THE WEATHER FORECASTING SYSTEM OF POSEIDON

The weather forecasting system based on the SKIRON/Eta model is considered as the ''heart'' of the operational part of POSEIDON. For this reason, there is a need for making the entire system run both automatically and reliably. In order to achieve this, procedures have been developed to let the user control the run features of the basic model. The user specifies the model domain and the horizontal and vertical resolution of the model. These parameters are specified according to the specific needs and computational resources available. Also, the user defines the source of the meteorological data used for the initial and boundary conditions. Then, the time step (depending on horizontal resolution) and forecast period are specified as external parameters. After the input data are prepared, the whole system (sequence of different sub-programs) is executed by a procedure, which is activated at a specified time.

According to the needs of the POSEIDON operations, to downscale the weather conditions the system is executed twice with different model configurations. The first simulation is performed with the coarser resolution model (COARSE) in order to provide detailed initial and boundary conditions to the second model with the higher resolution (FINE). The two domains are illustrated in Fig. 1. In this figure, the letters A and B denote the COARSE and FINE model domains, respectively.

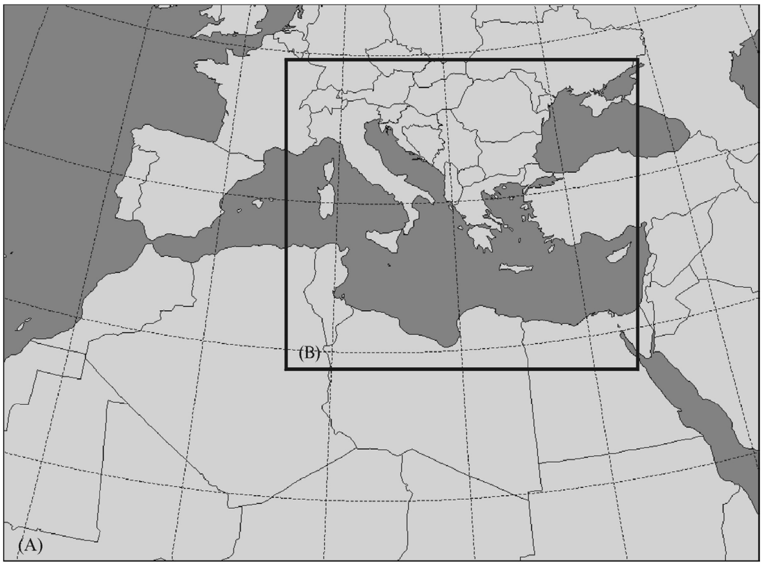

FIGURE 1 Model domains (A) COARSE and (B) FINE.

The COARSE version of the model has a horizontal grid increment of 0.24° while the geographical extension of the model domain is from 24.2°W to 51.8°E and from 12.9 to 53.4°N. In the vertical, 32 levels are used stretching from ground to the model top (15800 m). For the initial and the boundary meteorological conditions the NCEP objective analysis gridded data are used, in a 1.25° horizontal grid increment, for 10 standard pressure levels (1000, 850, 700, 500, 400, 300, 250, 200, 150 and 100 hPa). The above data set is downloaded daily from NCEP. The lateral boundaries of the model domain are updated at each time step from the NCEP data available every 6 h (linear interpolation). For SST, the NCEP 1-2-1 time filtered weekly data, at $1 \times 1°$ horizontal grid increment are used. The simulation period is 72 h.

The domain of the FINE version of the model extends from 2.6 to 38.4°E and from 27.4 to 49.5°N, with a horizontal grid increment of 0.10°. The distribution of the vertical layers is the same as in the COARSE model. The meteorological fields, as they produced by the COARSE model, provide the appropriate initial and the boundary meteorological conditions for the FINE model. Software has been developed in order to interpolate the meteorological fields from the COARSE to the FINE model grid points. In this way, the simulation with the FINE model is performed utilizing 24 standard pressure levels (1000, 980, 960, 940, 920, 900, 870, 850, 820, 770, 730, 700, 650, 600, 550, 500, 450, 400, 350, 300, 250, 200, 150 and 100 hPa) and updates its boundary conditions every 1 h. For SST, the same gridded data from NCEP are used. The length of the simulation is the same as in the COARSE model (i.e. 72 h).

The entire system has been designed to operate in an optimum way. Both versions of the model perform their simulation simultaneously. While the COARSE model performs its own simulation, the preprocessor of the FINE model prepares the appropriate fields in order to feed the FINE execution of the model, when the necessary output is ready. The flow charts of all the operations for the weather forecasting system of POSEIDON are shown in Fig. 2.

3.1 Comparison of Model Results Against Buoys Measurements

The atmospheric model of the POSEIDON system is run automatically according to the procedure described previously. An evaluation system has been developed and used for quality control of the results provided to the other parts (e.g. wave, ocean circulation and oil spill models etc). The evaluation scheme consists of various statistical tests. The data used are selected from the POSEIDON buoy network.

The estimated fields of wind speed, air temperature and mean sea level pressure are verified using the point measurements of the buoys. The model values were interpolated to each observation site using the simple bilinear interpolation expression:

$$M = \frac{\sum_{k=1}^{4} w_k \cdot M_k}{\sum_{k=1}^{4} w_k} \tag{21}$$

where M_k are the model values at the four model grid points surrounding the observation. The weighting factor w_k is defined in such a way that the nearest points have the

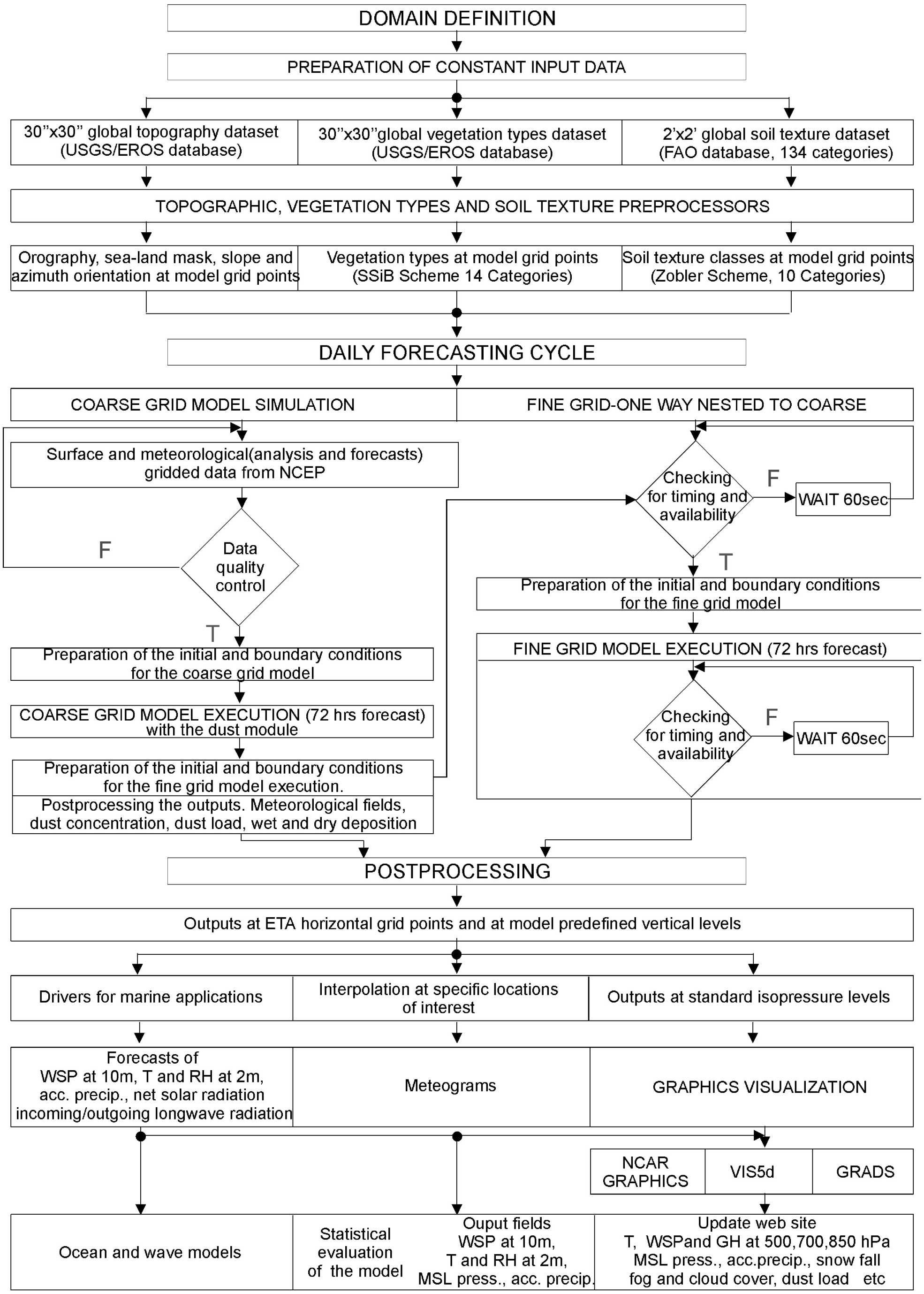

FIGURE 2 Flow chart for the operational processes.

most influence and is given by:

$$w_k = \frac{1}{r_k^2} \tag{22}$$

where r_k is the distance from the k model grid point to the observation.
The three basic statistical measures suggested by Wilks (1995), mean error (BIAS), root mean square error (RMSE) and correlation coefficient (r) are calculated. In addition, the absolute skill score SCORE_a was used to assess the forecast performance. Using the measure SCORE_a the forecast accuracy of the value M against observation O is computed by:

$$\text{SCORE}_a = 100 \cdot \left(1 - \frac{1}{N} \cdot \sum_{i=1}^{N} \left|\frac{M_i - O_i}{O_i}\right|\right) \tag{23}$$

Due to the fact that the buoys are located close to coastline, the point-to-point comparison between model values and observations faces a difficulty arising from the characterization of the model grid points as land or sea points. As illustrated in Fig. 3, the red bullets denote the locations of the buoys in Aegean Sea and the green and blue ones the corresponding four neighbour model grid points, characterizing the land and the sea points, respectively. For instance, for the buoy location at the island Dia, north of Crete, in order to compute the interpolated values using the expression (21) two different situations arise. Using the COARSE model mesh values from three land and one sea grid point are used, while from the FINE model mesh values from four sea grid points are used. Plotting the time series of the estimated air temperature, together with the corresponding observations, it is evident that the diurnal temperature variation is more intense when the COARSE model values are used (Fig. 4).

(a) **(b)**

FIGURE 3 Locations of buoys (red bullets) and the corresponding four neighbor model grid points for (a) the COARSE and (b) the FINE configuration. Green bullets denote the land grid points and the blue ones the sea points.

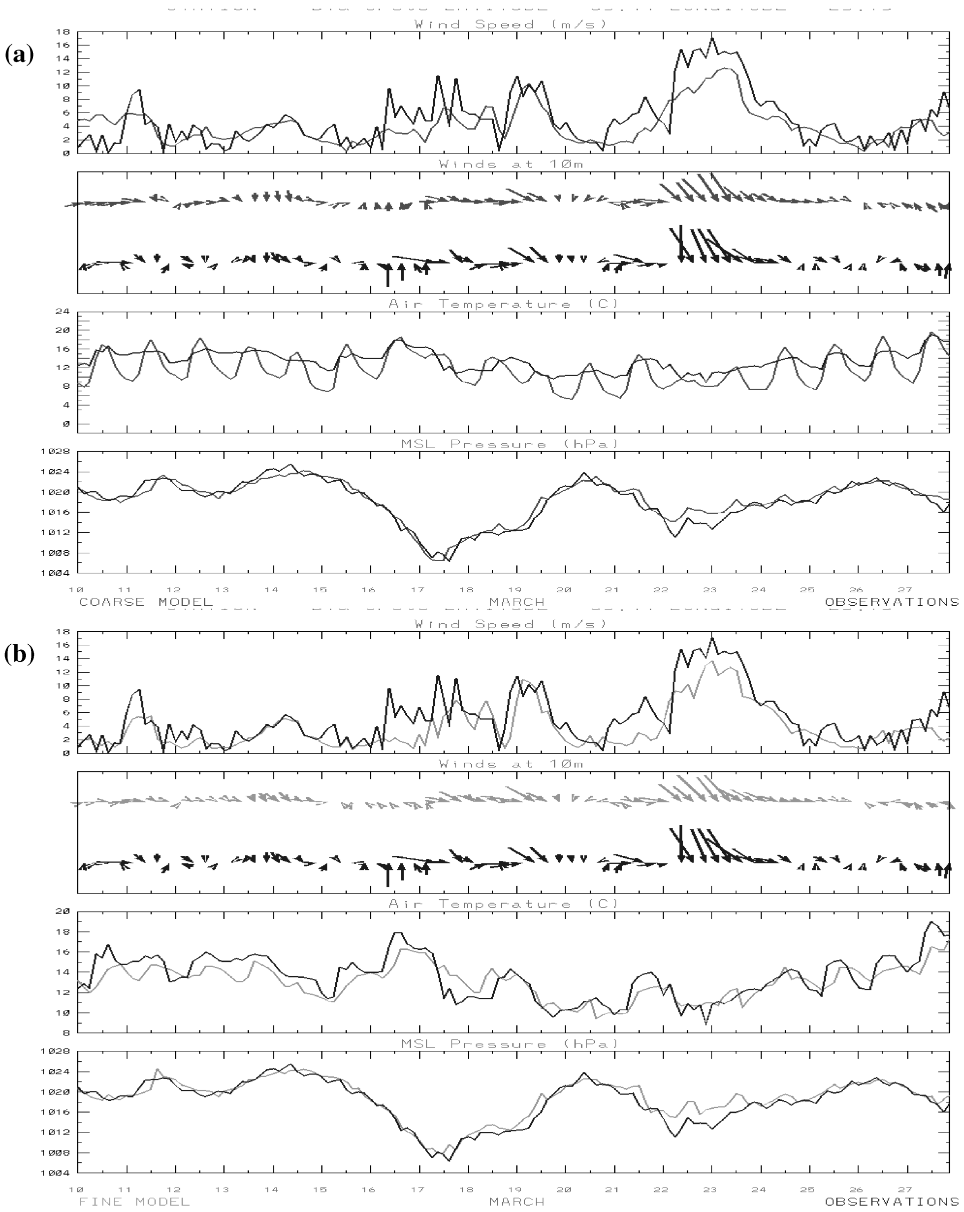

FIGURE 4 Time series of measurements of buoys and (a) COARSE and (b) FINE model estimations for wind speed and direction, air temperature and mean sea level pressure for the buoy near the Dia island (Crete).

The sampling period for the statistical evaluation is 12 months (1 April 2000–31 March 2001). For this period, model forecasts for both COARSE and the FINE model configuration were interpolated at the buoy locations and were compared with the observations. The time series created are relatively complete, since there are almost no missing cases in the model runs but there are some buoy data missing due to various reasons (instrument malfunction, drifting or change in location). The results

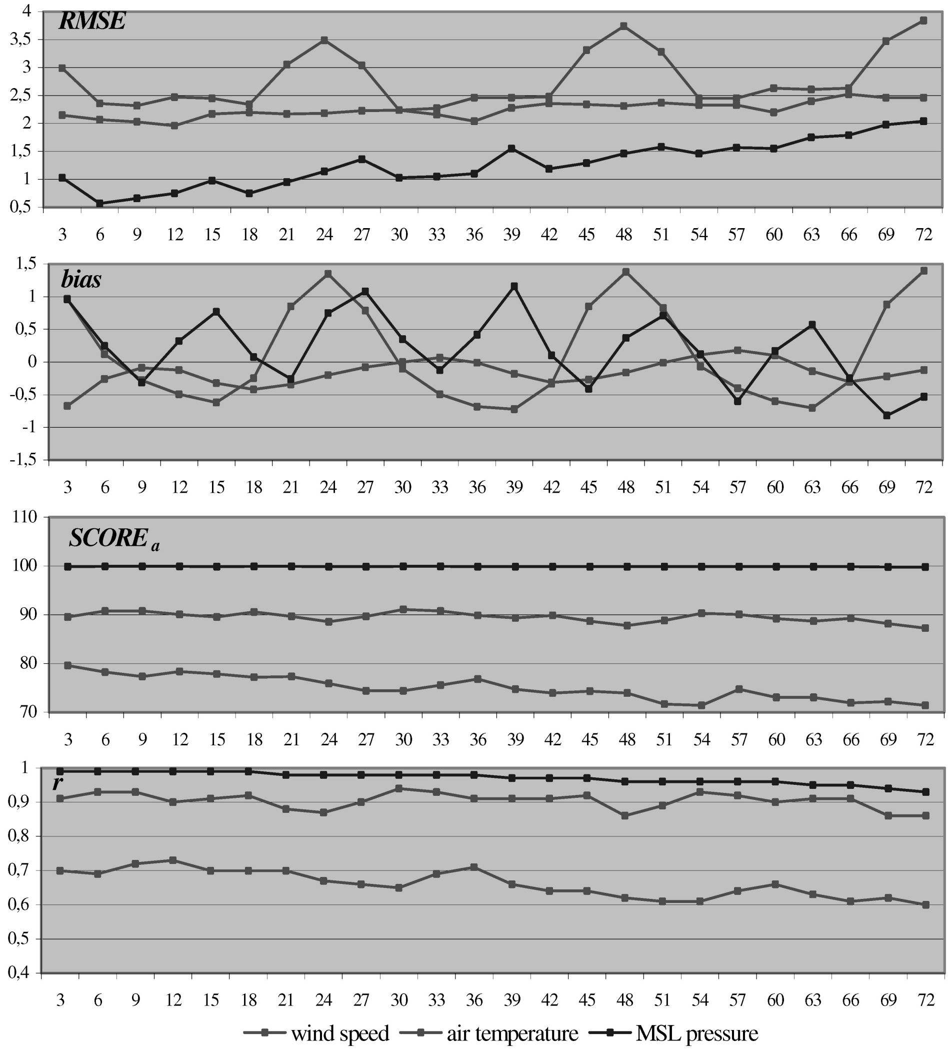

FIGURE 5 Statistical scores for the COARSE model grid. The horizontal axis is hours of forecast. The evaluation period is from 1 April 2000 through 31 March 2001.

of the analysis are showed in Figs. 5 and 6. Both model configurations perform quite satisfactorily, despite the fact that gridded forecasting fields are compared with point-measured fields. Differences between the fields are between the sampling (and averaging) periods in the buoy data (average of the last 10 min) and the model time step. It is noticeable that the performance of the models remains satisfactory almost in the entire 72 h integration. Comparing the performance of COARSE and FINE model configuration it is evident that using the higher resolution there is a significant improvement especially in the estimation of air temperature and therefore, fluxes (not shown here). With this verification based on point measurements, the advantages from the use of higher resolution are not clearly shown. For instance, due to the vectorial nature of the wind the composition of the four neighbour wind vectors leads to an

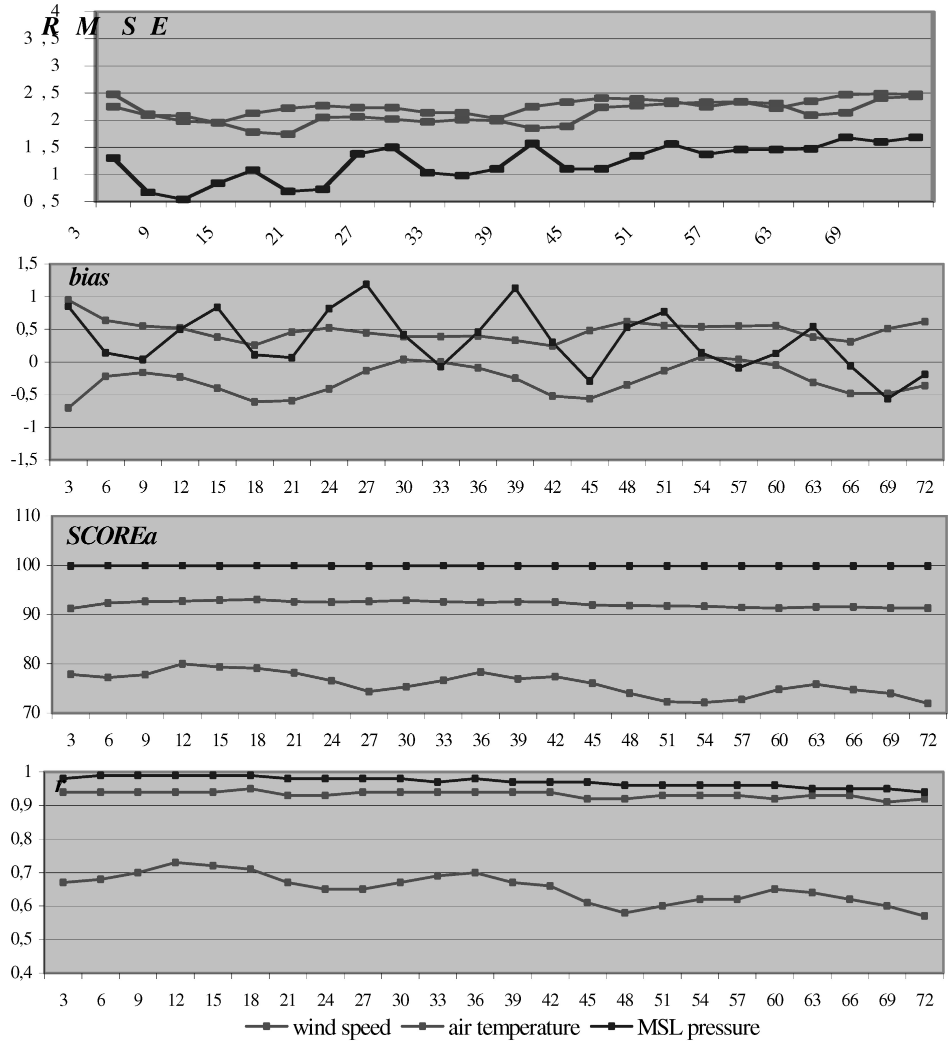

FIGURE 6 Statistical scores for the FINE model grid. The horizontal axis is hours of forecast. The evaluation period is from 1 April 2000 through 31 March 2001.

underestimation of the magnitude of the resultant vector. Despite this fact, the advantages of using a smaller grid increment are more clear when the hydrodynamic model and wave model use the atmospheric forcing from the FINE model.

3.2 Evaluation of the Dust Module of the SKIRON/Eta Model

Currently the simulation of the dust cycle in the atmosphere is performed within the integration of the COARSE version of the weather forecasting system of POSEIDON. In each day run, the initial state of dust concentration in the atmosphere is computed from the previous-day model run.

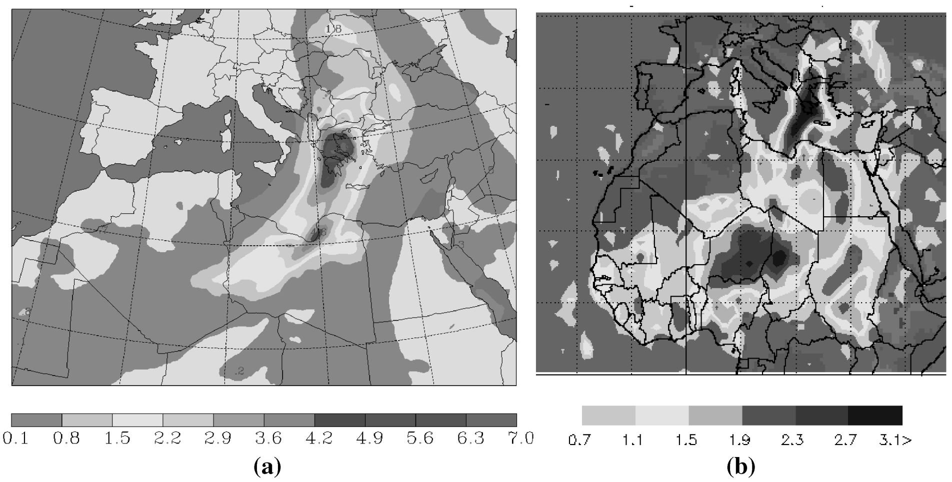

FIGURE 7 Transport of Saharan dust over Mediterranean Sea on 21 April 2000. (a) simulated dust load (in $g\,m^{-2}$) and (b) Aerosol-index calculated from data of TOMS satellite.

In the three years of the operation there is the opportunity to evaluate the dust transport against certain observational evidence. The lack of observed surface dust concentrations restricts the evaluation of the model results against satellite images only. For this purpose, the simulated dust load field is compared with the Aerosol Index (AI) – the parameter that describes the level of UV absorption due to the existence of dust and smoke in the atmosphere (Herman *et al.*, 1996). Despite the fact that there is no straightforward way to convert dust load to AI, the comparison of the position and shapes of the two fields may be used for a quality control of the dust model performance (Fig. 7).

4. CONCLUSION

In this presentation, a general description of the weather forecasting system of POSEIDON has been discussed. The system is designed so that it can be used successfully for both, research and routine weather forecasting. The implementation of new features in the parameterization of the surface processes (Papadopoulos *et al.*, 1997), the radiative transfer scheme and the application of the one-way nested grid technique, enhance the capability of the system to simulate with considerable success small scale processes in the atmosphere. It can accurately simulate extreme weather phenomena and natural hazards associated with them (Kallos *et al.*, 1998a,b). Over the sea, the implementation of viscous sublayer allows the improvement of the description of the atmospheric state close to the surface and the air–water exchange processes. In addition to these, the COARSE version is able to simulate the dust cycle (uptake-transport-deposition) in an accurate way. Finally, the system is able to run operationally on relatively cheap computer platforms in an efficient way.

The weather forecasting system of POSEIDON is operating in its COARSE version since February 1999 and in its FINE version since September 1999. Therefore, there is the opportunity for it to be tested in a number of severe weather situations. In order to evaluate the model performance over sea, a comparison against the measured fields from the buoy network of the POSEIDON system is performed. The entire performance of both versions of the system is quite satisfactory.

Acknowledgments

This work was performed with the support from the POSEIDON project funded by the Financial Mechanism of the European Economic Area (EFTA) and Greek Government. We would like to thank Dr G. Korres and Dr A. Lascaratos for the useful collaboration on coupling the two modeling systems. Finally, we would like to thank the anonymous reviewers as well as the Editor in Chief for their constructive comments.

References

Betts, A.K. (1986). A new convective adjustment scheme. Part E: observational and theoretical basis. *Quart. J. R. Met. Soc.*, **112**, 677–691.

Betts, A.K. and Miller, M.J. (1986). A new convective adjustment scheme. Part II: single column tests using GATE wave, BOMEX, ATEX and Arctic Air mass data sets. *Quart. J. R. Met. Soc.*, **112**, 693–709.

Blumberg, A.F. and Mellor, G.L. (1983). Diagnostic and prognostic numerical circulation studies of the South Atlantic Bight. *J. Geophys. Res.*, **88**, 4579–4592.

Christopoulos, S. and Koutitas, C. (1991). Wave modeling in the North Aegean Sea. *Ann. Geophysicae*, **9**, 91–101.

Dulac, F., Jankowiak, I., Legrand, M., Tanre, D., N'Doume, C.T., Guillard, F., Lardieri, D., Guelle, F. and Poitou, J. (1994). Meteosat imagery for quantitative studies of Saharan dust transport. *Proc. Meteosat Scientific Users Meeting*. 5–9 September, Cascais, Portugal.

Herman, J.R., Bhartia, P.K., Torres, O., Hsu, C., Seftor, C. and Celarier, E. (1996). Global distribution of UV-absorbing aerosols from Nimbus-7/TOMS data. *J. Geophys. Res.*, **102**, 16911–16929.

Janjic, Z.I. (1974). A stable centered difference scheme free of the two-grid-interval noise. *Mon. Wea. Rev.*, **102**, 319–323.

Janjic, Z.I. (1979). Forward–backward scheme modified to prevent two-grid-interval noise and its application in sigma coordinate models. *Contrib. Atmos. Phys.*, **52**, 69–84.

Janjic, Z.I. (1984). Non-linear advection schemes and energy cascade on semi-staggered grids. *Mon. Wea. Rev.*, **112**, 1234–1245.

Janjic, Z.I. (1990). The step-mountain coordinate: physical package. *Mon. Wea. Rev.*, **118**, 1429–1443.

Janjic, Z.I. (1994). The step-mountain Eta coordinate model:further developments of the convection, viscous sublayer and turbulence closure schemes. *Mon. Wea. Rev.*, **122**, 927–945.

Kallos, G., Nickovic, S., Papadopoulos, A., Jovic, D., Kakaliagou, O., Misirlis, N., Boukas, L., Mimikou, N., Sakellaridis, G., Papageorgiou, J., Anadranistakis, E. and Manousakis, M. (1997a). The regional weather forecasting system SKIRON: an overview. *Proceedings of the International Symposium on Regional Weather Prediction on Parallel Computer Environments*, (15–17 October 1997). pp. 109–122. Athens, Greece.

Kallos, G., Nickovic, S., Jovic, D., Kakaliagou, O., Papadopoulos, A., Misirlis, N., Boukas, L., Mimikou, N., Sakellaridis, G., Papageorgiou, J., Anadranistakis, E. and Manousakis, M. (1997b). The regional weather forecasting system SKIRON and its capability for forecasting dust uptake and transport. *Proceedings of WMO Conference on Dust Storms*, (1–6 November 1997). pp. 9. Damascus, Syria.

Kallos, G., Papadopoulos, A., Nickovic, S., Katsafados, P. and Kakaliagou, O. (1998a). Forecasting extreme rainfall events in the Mediterranean region with the SKIRON system: sensitivity tests. *6th International Conference on Precipitation: Predictability of Rain at the Various Scales*, 29 June–1 July 1998. Hawaii, USA.

Kallos, G., Papadopoulos, A., Nickovic, S. and Katsafados, P. (1998b). The regional weather forecasting models as predictive tools for major environmental disasters and natural hazards. *5th NATO/ARW workshop on Large Scale Computations in Air Pollution Modeling*, 6–10 July 1998. Sofia, Bulgaria.

Komen, G.J., Cavaleri, L., Donelan, M., Hasselmann, K., Hasselmann S. and Janssen, P.A.E.M. (1994). *Dynamics and Modeling of Ocean Waves*, 532pp. Cambridge University Press, Cambridge, England.

Korres, G., Lascaratos, A. and Hatziapostolou, H. (2002). Towards an ocean forecasting system for the Aegean Sea. GAOS (in this issue).
Liu, W.T., Katsaros, K.B. and Businger, J.A. (1979). Bulk parametrization of air–sea exchanges of heat and water vapor including the molecular constraints at the interface. *J. Atmos. Sci.*, **36**, 1722–1735.
Lobocki, L. (1993). A procedure for the derivation of surface-layer bulk relationships from simplified second order closure models. *J. Appl. Meteor.*, **32**, 126–138.
Mangarella, P.A., Chambers, A.J., Street, R.L. and Hsu, E.Y. (1973). Laboratory studies of evaporation and energy transfer through a wavy air–water interface. *J. Phys. Oceanogr.*, **3**, 93–101.
Mellor, G.L. and Yamada, T. (1974). A hierarchy of turbulence closure models for planetary boundary layers. *J. Atmos. Sci.*, **31**, 1791–1806.
Mellor, G.L. and Yamada, T. (1982). Development of a turbulence closure model for geophysical fluid problems. *Rev. Geophys, Space Phys.*, **20**, 851–875.
Mesinger, F. (1973). A method of construction of second order accuracy difference schemes permitting no false two-grid interval wave in the height field. *Tellus*, **25**, 444–458.
Mesinger, F. (1977). Forward–backward scheme and its use in a limited area model. *Contrib. Atmos. Phys.*, **50**, 200–210.
Mesinger, F. (1984). A blocking technique for representation of mountains in atmospheric models. *Riv. Meteor. Aeronaut.*, **44**, 195–202.
Mesinger, F., Janjic, Z.I., Nickovic, S., Gavrilov, D. and Deaven, D.G. (1988). The steep-mountain coordinate: model description and performance for cases of Alpine lee cyclogenesis and for a case of an Appalachian redevelopment. *Mon. Wea. Rew.*, **116**, 1493–1518.
Mihailovic, D. and Kallos, G. (1997). A sensitivity study of a coupled soil-vegetation boundary layer scheme for use in mesoscale modeling. *Boundary-Layer Meteorol.*, **82**, 283–315.
Monin, A.S. and Obukhov, A.M. (1954). Osnovnye zakonomernosti turbulentnogo peremeivani v prizemnem sloie atmosfery. *Trudy Geofiz. in-ta AN SSSR*, **24**(151), 163–187.
Nickovic, S. and Dobricic, S. (1996). A model for long-range transport of desert dust. *Mon. Wea. Rev.*, **124**, 2537–2544.
Nickovic, S., Jovic, D., Kakaliagou O. and Kallos, G. (1997a). Production and long-range transport of desert dust in the Mediterranean region: Eta model simulations. *22nd NATO/CCMS International Technical Meeting on Air Pollution Modeling and Its Applications*, 2–6 June 1997. Clermont-Ferrand, France.
Nickovic, S., Kakaliagou, O., Kallos, G., Jovic, D. and Papadopoulos, A. (1997b). Eta/dust model: sensitivity to model resolution and desert source specification. *First International Symposium on Sand and Dust Storms*, 2–7 November. Damascus, Syria.
Nickovic, S., Kallos, G., Papadopoulos, A. and Kakaliagou, O. (2001). A model for prediction of desert dust cycle in the atmosphere. *Journal of Geophysical Research*, **106**(D16), 18113–18129.
Papadopoulos, A., Kallos, G., Nickovic, S., Jovic, D., Dacic M. and Katsafados, P. (1997). Sensitivity studies of the surface and radiation parameterization schemes of the SKIRON system. *Proceedings of the International Symposium on Regional Weather Prediction on Parallel Computer Environments*, 15–17 October 1997. 155–164, Athens, Greece.
Paulson, C.A. (1970). The mathematical representation of wind speed and temperature profiles in the unstable atmospheric surface layer. *J. Appl. Meteor.*, **9**, 857–861.
Wilks, D.S. (1995). *Statistical Methods in the Atmospheric Sciences: An Introduction*, 467pp. Academic Press, San Diego, California.